Available online at www.sciencedirect.com
ScienceDirect
Bioorganic & Medicinal Chemistry Letters 18 (2008) 2739–2744
Bioorganic & Medicinal Chemistry Letters

Synthesis and SAR of new pyrrolo[2,1-*f*][1,2,4]triazines as potent p38α MAP kinase inhibitors

Stephen T. Wrobleski,[a,*] Shuqun Lin,[a] John Hynes, Jr.,[a] Hong Wu,[a] Sidney Pitt,[b] Ding Ren Shen,[b] Rosemary Zhang,[b] Kathleen M. Gillooly,[b] David J. Shuster,[b] Kim W. McIntyre,[b] Arthur M. Doweyko,[c] Kevin F. Kish,[c] Jeffrey A. Tredup,[c] Gerald J. Duke,[c] John S. Sack,[c] Murray McKinnon,[b] John Dodd,[a] Joel C. Barrish,[a] Gary L. Schieven[b] and Katerina Leftheris[a]

[a]*Department of Immunology Chemistry, Bristol-Myers Squibb, Princeton, NJ 08543-4000, USA*
[b]*Department of Immunology Drug Discovery, Bristol-Myers Squibb, Princeton, NJ 08543-4000, USA*
[c]*Department of Structural Biology and Modeling, Bristol-Myers Squibb, Princeton, NJ 08543-4000, USA*

Received 12 November 2007; revised 22 February 2008; accepted 27 February 2008
Available online 4 March 2008

Abstract—A novel series of compounds based on the pyrrolo[2,1-*f*][1,2,4]triazine ring system have been identified as potent p38α MAP kinase inhibitors. The synthesis, structure–activity relationships (SAR), and in vivo activity of selected analogs from this class of inhibitors are reported. Additional studies based on X-ray co-crystallography have revealed that one of the potent inhibitors from this series binds to the DFG-out conformation of the p38α enzyme.

The lack of convenient and effective treatments for chronic debilitating inflammatory diseases such as rheumatoid arthritis, Crohn's disease, and psoriasis represents a significant unmet medical need. The recent success of the anti-cytokine biological agents anakinra (Kineret),[1] an IL-1 receptor antagonist, etanercept (Enbrel),[2] a soluble TNF receptor fusion protein, and infliximab (Remicade)[3] and adalimumab (Humira), both TNF-α monoclonal antibodies, has demonstrated clinical benefit in the treatment of inflammatory diseases.[4] However, due to the well known disadvantages common to these protein-based therapies such as high cost and subcutaneous or intravenous administration, orally active small molecules that can effectively act as anti-cytokine agents would clearly be of added benefit to patients.[5]

The p38 mitogen-activated protein kinase (MAPK) pathway has been proven to play a central role in the regulation of the proinflammatory cytokines TNF-α and IL-1β.[6] The p38 MAPK family consists of four isoforms (α, β, γ, and δ) whereby p38α is believed to be the predominant isoform involved in the inflammatory response.[7] As a result, the development of orally active small molecule p38α inhibitors has been actively pursued by many researchers.[8] In collaboration with others, we previously identified and reported substituted triaminotriazines[9] and 5-cyanopyrimidines[10] as novel and potent p38α inhibitors. In an ongoing effort to identify structurally diverse analogs, we have recently discovered a series of substituted pyrrolo[2,1-*f*][1,2,4]triazines as novel inhibitors of the p38α MAP kinase.[11] This paper describes the synthesis and preliminary structure–activity relationships (SAR) of compounds based on the general structure depicted in Figure 1 where modifications of the R^1 and R^2 substituents have recently been evaluated. In addition, results from X-ray co-crystallographic studies of an analog bound to unphosphorylated p38α and in vivo evaluation of select compounds in a murine model of acute inflammation will be discussed.

Exploration of the C-6 SAR used analog **1** as a starting point based on published work from our own laboratories and those of others.[12,13] Using the route previously reported,[12] the synthesis began with the known pyrrole

Keywords: p38; Kinase; Inflammation; Pyrrolotriazines; TNF-α; IL-1.
* Corresponding author. Tel.: +1 609 252 4873; fax: +1 609 252 6601; e-mail: stephen.wrobleski@bms.com

0960-894X/$ - see front matter © 2008 Elsevier Ltd. All rights reserved.
doi:10.1016/j.bmcl.2008.02.067

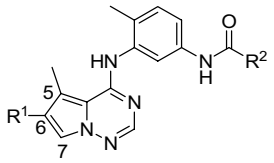

Figure 1. General structure of new pyrrolo[2,1-*f*][1,2,4]triazine based p38α inhibitors.

2[14] (Scheme 1). Deprotonation with NaH and reaction with either *O*-(2,4-dinitrophenyl)hydroxylamine or monochloramine[15] followed by cyclization with formamide provided intermediate **3**. Subsequent chlorination using $POCl_3$ afforded **4** which was coupled with various functionalized anilines **5** to yield intermediate **6**. Finally, hydrolysis of the C-6 ester and amide formation under standard conditions provided the desired analogs **7** for initial evaluation using in vitro assays.[16]

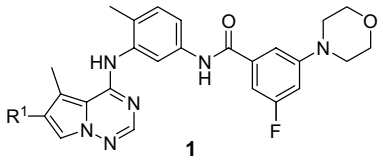

1

The C-6 SAR showed that the most active compounds at inhibiting the enzyme contained either a primary or secondary amide (**11**–**17**, **20**), an ester (**9**), or a carboxylic acid (**10**) (Table 1). The tertiary amide **19** and the C-6 unsubstituted pyrrolotriazine **8** had decreased potency relative to these analogs. In addition, the (*S*)-enantiomer of the α-methylbenzyl amide (**17**) was nearly 50-fold more potent against p38α than the corresponding (*R*)-enantiomer (**18**). At the time, this finding suggested to us that the α-methylbenzyl group might be occupying a lipophilic pocket in the p38α active site that had been utilized by other reported p38 inhibitors containing a similar preference for the (*S*)-α-methylbenzyl group over its enantiomeric counterpart.[17] This hypothesis was later validated by X-ray co-crystallographic studies of a closely related analog to **17** (vide infra).

Having identified a series of analogs with potent inhibitory activity against the enzyme, the compounds were subsequently evaluated for inhibition of TNF-α release in human peripheral blood mononuclear cells (PBMCs).[16] With the exception of the carboxylic acid **10**, the cellular potency correlated well with the enzyme inhibition potency. The most active compounds in cells included the ethyl amide **13** and the (*S*)-α-methylbenzylamide **17** which were equipotent at TNF-α inhibition (IC_{50} = 2 nM). Lack of cellular activity for the acid **10** was likely due to poor cell permeability.

To evaluate the aryl amide SAR, the C-6 position was fixed using the (*S*)-α-methylbenzyl amide (Table 2). Substitution at the meta or para positions of the aryl ring generally provided the most potent compound.

The optimal substituents were found to be the 4-cyano (**27**) and the 3-morpholino (**28**, **30**) groups along with the previously identified 3-fluoro, 5-morpholino disubstitution pattern (**17**). The unsubstituted analogs **21** and **29** and the 3-methyl substituted compound **22** had slightly decreased potency whereas the 3,5-disubstituted CF_3 analog **25** and 2,6-dichloro analog **26** did not show significant activity when tested up to 1 μM. In addition, replacement of the phenyl ring with a 4-pyridyl group provided equipotent analogs against the enzyme, albeit, with a slightly decreased cellular activity relative to their phenyl ring counterparts (**21** vs **29** and **28** vs **30**).

Replacement of the morpholine group with other heterocycles was also investigated in the C-6 ethyl amide series (Table 3). Incorporation of an *N*-methyl piperazine ring (**32**) or five-membered heteroaromatic groups (**33**, **34**) resulted in reduced enzymatic potency relative to the morpholine substitution (**31**). Although the imidazole analog **34** and the γ-lactam **27** did have respectable enzymatic potency in the nanomolar range, the cellular potency for both compounds was >100 nM. As a result, these compounds were not further investigated.

Combination of the optimal pyrrolotriazine C-6 substituents and aryl amide side chain substituents provided the most potent compounds as summarized in Table 4. In addition, the (*S*)-1-methoxy-2-propan-2-yl C-6 amides **38**–**40** were also prepared. Although these derivatives were slightly less potent than the ethyl and α-methylbenzyl amides in most cases, they did show

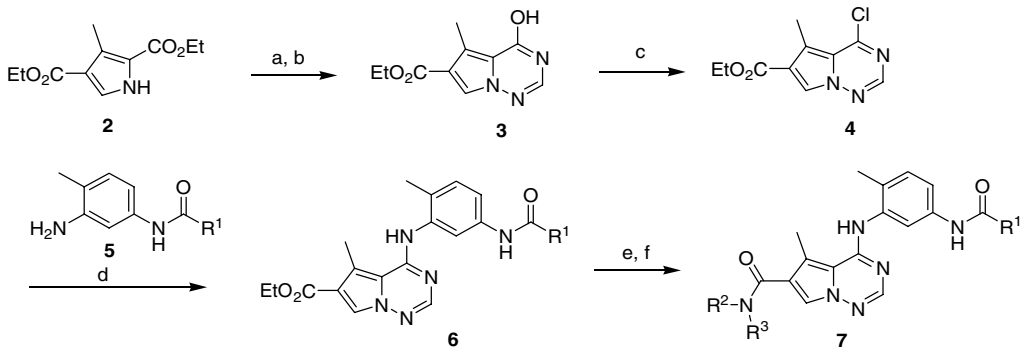

Scheme 1. Synthesis of pyrrolo[2,1-*f*][1,2,4]triazine based p38 inhibitors. Reagents and conditions: (a) NaH, DMF then $DnpONH_2$ or NH_2Cl in Et_2O; (b) formamide, 165 °C; (c) $POCl_3$, 110 °C; (d) DMF, 55 °C; (e) 1 N aq NaOH, THF, 50 °C; (f) R^2R^3NH, EDCI, HOBt, DMF.

Table 1. Pyrrolotriazine C-6 SAR

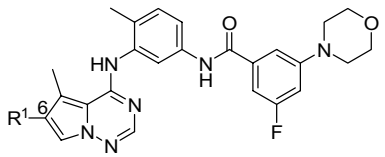

Compound	R^1	p38α IC_{50} (nM)	TNFα IC_{50} (nM)
8	H	27	98
9	$–CO_2Et$	2	4
10	$–CO_2H$	1	>1000
11	$–C(O)NH_2$	3	19
12	–C(O)NHMe	4	14
13	–C(O)NHEt	0.42[a]	2
14	–C(O)NH-*n*-Pr	5	4
15	–C(O)NH-*i*-Pr	5	6
16	–C(O)NH-(*S*)-1-methoxy-2-propan-2-yl	2	7
17	–C(O)NH-(*S*)-α-methylbenzyl	0.54[a]	2
18	–C(O)NH-(*R*)-α-methylbenzyl	23	48
19	$–C(O)N(Me)_2$	63	212
20	$–C(O)NHCH_2CH_2N(Me)_2$	10	18

[a] K_i determination.

Table 2. Aryl amide side chain SAR

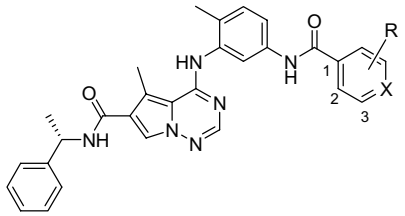

Compound	R	X	p38α IC_{50} (nM)	TNFα IC_{50} (nM)
21	H	C	19	52
22	3-Methyl	C	94	259
23	4-Methyl	C	13	313
24	$3-CF_3$	C	32	72
25	$3,5-Di-CF_3$	C	>1000	—
26	2,6-Dichloro	C	>1000	—
27	4-Cyano	C	3.40[a]	11
28	3-Morpholino	C	0.46[a]	29
17	3-F, 5-Morpholino	C	0.54[a]	2
29	H	N	14	117
30	3-Morpholino	N	0.44[a]	43

[a] K_i determination.

slightly improved aqueous solubility relative to the other derivatives (data not shown). Unfortunately, this improved aqueous solubility did not translate into improved cellular activity.

To gain insight into the binding mode of this novel series of p38 inhibitors, an X-ray crystal structure of analog **30** co-complexed with purified, unphosphorylated p38α was solved.[18] The key binding interactions between **30** and the p38α enzyme are illustrated in Figure 2. Four hydrogen bonds are apparent between the inhibitor and the protein. These include two hydrogen bonds from the pendant diaryl amide linker to Glu71 and Asp168 and a hydrogen bond between the pyrrolotriazine N1 and Leu171 residue. In addition, a key hydrogen bond between the pyrrolotriazine C6-amide carbonyl and the p38α hinge region Met109 residue is also observed. The coplanar orientation of the C-6 amide and pyrrolotriazine ring system in the bound state explains the decreased activity of the C6-tertiary amide **19** which most likely prefers a nonplanar orientation. Further analysis of the co-complex reveals that the binding of **30** requires a large protein conformational change in the conserved Asp-Phe-Gly (DFG) motif to accommodate the morpholino group. This protein conformation has been commonly referred to as the DFG-out conformation[19] and allows the morpholine group to occupy a large hydrophobic pocket normally occupied by the Phe169 side chain. The presence of the morpholine group in this lipophilic pocket lined by the hydrophobic residues Leu74, Leu75, Val83, Ile141, Ile146, and Ile166 (not shown) explains why most analogs lacking this group are significantly less potent. In addition, compounds containing groups larger than a fluorine on opposite sides of the phenyl ring (**25**, **26**) are significantly less potent (>1 μM) presumably due to unfavorable interactions with the Glu71 side chain which is positioned on the opposite side of the phenyl ring relative to the lipophilic pocket. While the decreased potency of the piperazine analog **32** can easily be rationalized

Table 3. Heterocycle modifications

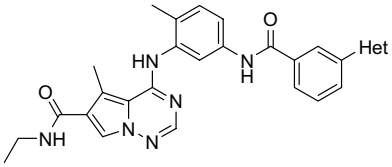

Compound	Het	p38α IC_{50} (nM)	TNFα IC_{50} (nM)
31		0.98[a]	45
32	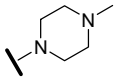	924	—
33		123	—
34		7	126
35		16	633

[a] K_i determination.

Table 4. Optimal pyrrolotriazine C6 substituents with optimal aryl amide substitutions

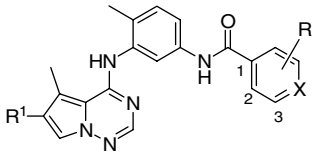

Compound	R^1	X	R	p38α IC_{50} (nM)	TNFα IC_{50} (nM)
31	–C(O)NHEt	C	3-Morpholino	0.98[a]	45
36	–C(O)NHEt	N	3-Morpholino	2	287
13	–C(O)NHEt	C	3-F, 5-Morpholino	0.42[a]	2
37	–C(O)NHEt	C	4-Cyano	23	46
38	–C(O)NH-(*S*)-1-methoxy-2-propan-2-yl	C	3-Morpholino	12	29
39	–C(O)NH-(*S*)-1-methoxy-2-propan-2-yl	C	3-F, 5-Morpholino	2	7
40	–C(O)NH-(*S*)-1-methoxy-2-propan-2-yl	C	4-Cyano	16	65
28	–C(O)NH-(*S*)-α-methylbenzyl	C	3-Morpholino	0.46[a]	2
30	–C(O)NH-(*S*)-α-methylbenzyl	N	3-Morpholino	0.44[a]	18
17	–C(O)NH-(*S*)-α-methylbenzyl	C	3-F, 5-Morpholino	0.54[a]	2
27	–C(O)NH-(*S*)-α-methylbenzyl	C	4-Cyano	3.4[a]	6

[a] K_i determination.

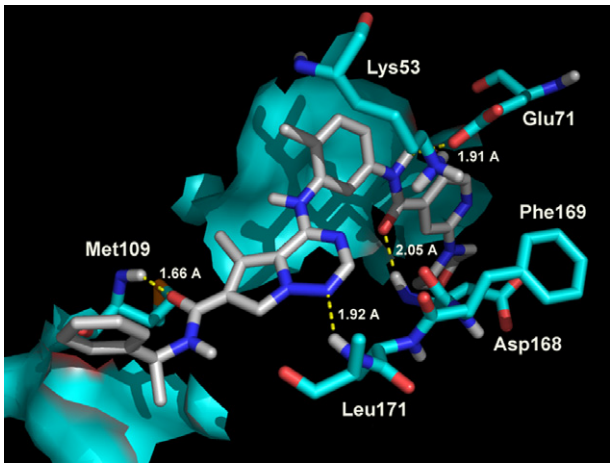

Figure 2. Binding interactions between **30** and unphosphorylated p38α based on X-ray crystallographic analysis (2.4 Å resolution, PDB entry 3BV2). Hydrogen-bond distances are given in angstroms with key protein residues labeled.

by noting that a protonated amine would not be favored in the lipophilic pocket, the potency differences between analogs **33**, **34**, and **35** could not be easily explained based on the X-ray structure of **30**. In addition, a rationale for the significant in vitro potency of the 4-cyano substituted analogs which lacked the morpholino group (**27**, **37**, **40**) could not be gleaned from the structure of **30**. These compounds would not be expected to bind to the DFG-out conformation since they do not contain a large lipophilic substituent normally required to displace the Phe169 side chain.

Other interesting features from the co-complex with **30** include the placement of the *ortho*-methyl substituted phenyl ring within the hydrophobic selectivity pocket and the orientation of the chiral α-methylbenzyl group against a hydrophobic surface near the edge of the binding site, consistent with other reported p38α inhibitors that contain this moiety.[17] In addition, an indirect hydrogen bond between the pyrrolotriazine N-3 and the Lys53 may be possible through the intermediacy of a water molecule (not shown). Finally, it is also apparent from this structure that the DFG-out protein conformation nicely accommodates a unique H-bond between the pyrrolotriazine N1 of **30** and the Leu171 residue. Interestingly, this is in contrast to the reported binding mode of structurally related quinazoline-based p38 inhibitors where the quinazoline core orients differently within the active site to form a direct hydrogen bond between the quinazoline N1 and the hinge region Met109 residue.[20]

All compounds having significant cellular potency (IC_{50} < 100 nM) were tested by oral administration in an acute in vivo murine model where the inhibition of LPS-stimulated TNF-α production was measured. Compounds **28**, **30**, and **31** were found to be the most potent in this model, significantly inhibiting TNF-α production by 87%, 89%, and 84%, respectively (Fig. 3).

In conclusion, we have developed a novel series of pyrrolo[2,1-*f*][1,2,4]triazine p38α MAP kinase inhibitors having potent activity against the enzyme. Derivatives **28**, **30**, and **31** show significant inhibition of LPS-stimulated TNF-α production when orally administered in an in vivo murine model. X-ray crystallographic studies of compound **30** show that the inhibitor binds to the DFG-out protein conformation and forms hydrogen-bond interactions with key residues (Met109, Glu71, and Asp168) that have been utilized by other reported p38α inhibitors.[21] Despite these similarities, the pyrrolotriazine inhibitors such as **30** are unique in that they bind to p38α in an orientation that is significantly different than the structurally related quinazoline-based inhibitors. In addition, the pyrrolotriazine N1 in the case of **30** forms a unique hydrogen-bond interaction

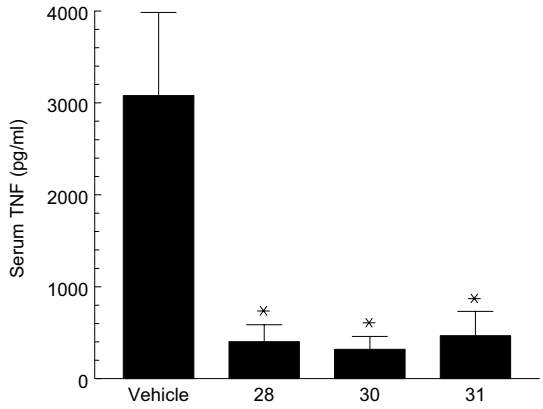

Figure 3. LPS-induced TNF-α inhibition by **28**, **30**, and **31** in mouse. BALB/c female mice (Harlan), 6–8 weeks of age, were used. Compounds were dosed (10 mg/kg) in poly(ethylene glycol) (MW = 300; PEG 300) to mice (n = 8/treatment) by oral gavage in a volume of 0.1 mL. Control mice received PEG300 alone ('Vehicle'). Thirty minutes later, mice were injected intraperitoneally with 50 μg/kg lipopolysaccharide (LPS; *E. coli* O111:B4; Sigma). Blood samples were collected 90 min after LPS injection. Serum was separated and analyzed for the level of TNF-α by commercial ELISA assay (BioSource) according to the manufacturer's instructions. Data shown are means ± SD. $^{*}p < .05$ versus Vehicle, ANOVA. Positive control (compd **11b** from Ref. 11) gave 95% TNF-α inhibition in this assay.

with the Leu171 residue. Future efforts to further explore the promising potential of pyrrolo [2,1-*f*][1,2,4]triazines as p38α MAP kinase inhibitors will be reported in due course.

Acknowledgments

We, the authors, thank our colleagues Dr. Brian E. Fink, Dr. Kyoung S. Kim, and Dr. Alaric D. Dyckman for helpful suggestions in the preparation of this manuscript.

References and notes

1. (a) Kavanaugh, A. *Adv. Ther.* **2006**, *23*, 208; (b) Fleischmann, R. *Expert Rev. Clin. Immunol.* **2006**, *2*, 331.
2. Grunke, M.; Kalden, J. R. *Expert Rev. Clin. Immunol.* **2005**, *1*, 313.
3. (a) Saleem, B.; Mackie, S.; Emery, P. *Expert Rev. Clin. Immunol.* **2006**, *2*, 193; (b) Cottone, M.; Mocciaro, F.; Modesto, I. *Expert Opin. Biol. Ther.* **2006**, *6*, 401.
4. (a) Papadakis, K. A. *Expert Rev. Clin. Immunol.* **2006**, *2*, 11; (b) Mease, P. J. *Expert Opin. Biol. Ther.* **2005**, *5*, 1491; (c) Lee, S. J.; Kavanaugh, A. *Therapy* **2005**, *2*, 13.
5. Wagner, G.; Laufer, S. *Med. Res. Rev.* **2006**, *26*, 1.
6. (a) Adams, J. L.; Badger, A. M.; Kumar, S.; Lee, J. C. *Prog. Med. Chem.* **2001**, *38*, 1; (b) Lee, J. C.; Laydon, J. T.; McDonnell, P. C.; Gallagher, T. F.; Kumar, S.; Green, D.; McNulty, D.; Blumenthal, M. J.; Heyes, J. R. *Nature* **1994**, *372*, 739.
7. (a) Hale, K. K.; Trollinger, D.; Rihanek, M.; Manthey, C. L. *J. Immunol.* **1999**, *162*, 4246; (b) Allen, M.; Svensson, L.; Roach, M.; Hambor, J.; McNeish, J.; Gabel, C. A. *J. Exp. Med.* **2000**, *191*, 859; (c) Fearns, C.; Kline, L.; Gram, H.; Di Padova, F.; Zurini, M.; Han, J.; Ulevitch, R. J. *J. Leukocyte Biol.* **2000**, *67*, 705.
8. For reviews of this area see: (a) Hynes, J., Jr.; Leftheris, K. *Curr. Top. Med. Chem.* **2005**, *5*, 967; (b) Goldstein, D. M.; Gabriel, T. *Curr. Top. Med. Chem.* **2005**, *5*, 1017; (c) Diller, D. J.; Lin, T. H.; Metzger, A. *Curr. Top. Med. Chem.* **2005**, *5*, 953; (d) Dominguez, C.; Powers, D. A.; Tamayo, N. *Curr. Opin. Drug Disc. Dev.* **2005**, *8*, 421.
9. Leftheris, K.; Ahmed, G.; Chan, R.; Dyckman, A. J.; Hussain, Z.; Ho, K.; Hynes, J., Jr.; Letourneau, J.; Li, W.; Lin, S.; Metzger, A.; Moriarty, K. J.; Riviello, C.; Shimshock, Y.; Wen, J.; Wityak, J.; Wrobleski, S. T.; Wu, H.; Wu, J.; Desai, M.; Gillooly, K. M.; Lin, T. H.; Loo, D.; McIntyre, K. W.; Pitt, S.; Shen, D. R.; Shuster, D. J.; Zhang, R.; Diller, D.; Doweyko, A.; Sack, J.; Baldwin, J.; Barrish, J.; Dodd, J.; Henderson, I.; Kanner, S.; Schieven, G. L.; Webb, M. *J. Med. Chem.* **2004**, *47*, 6283.
10. Liu, C.; Wrobleski, S. T.; Lin, J.; Ahmed, G.; Metzger, A.; Wityak, J.; Gillooly, K. M.; Shuster, D. J.; McIntyre, K. W.; Pitt, S.; Shen, D. R.; Zhang, R. F.; Zhang, H.; Doweyko, A. M.; Diller, D.; Henderson, I.; Barrish, J. C.; Dodd, J. H.; Schieven, G. L.; Leftheris, K. *J. Med. Chem.* **2005**, *48*, 6261.
11. Hynes, J., Jr.; Dyckman, A. J.; Lin, S.; Wrobleski, S. T.; Wu, H.; Gillooly, K. M.; Kanner, S. B.; Lonial, H.; Loo, D.; McIntyre, K. W.; Pitt, S.; Shen, D. R.; Shuster, D. J.; Yang, X.; Zhang, R.; Behnia, K.; Zhang, H.; Marathe, P. H.; Doweyko, A. M.; Tokarski, J. T.; Sack, J. S.; Pokross, M.; Kiefer, S. E.; Newitt, J. A.; Barrish, J. C.; Dodd, J.; Schieven, G. L.; Leftheris, K. *J. Med. Chem.* **2008**, *51*, 4.
12. (a) Hunt, J. T.; Mitt, T.; Borzilleri, R.; Gullo-Brown, J.; Fargnoli, J.; Fink, B.; Han, W.-C.; Mortillo, S.; Vite, G.; Wautlet, B.; Wong, T.; Yu, C.; Zheng, X.; Bhide, R. *J. Med. Chem.* **2004**, *47*, 4054; (b) Fink, B. E.; Vite, G. D.; Mastalerz, H.; Kadow, J. F.; Kim, S.-H.; Leavitt, K. J.; Du, K.; Crews, D.; Mitt, T.; Wong, T. W.; Hunt, J. T.; Vyas, D. M.; Tokarski, J. S. *Bioorg. Med. Chem. Lett.* **2005**, *15*, 4774; (c) Borzilleri, R. M.; Zheng, X.; Qian, L.; Ellis, C.; Cai, Z.-W.; Wautlet, B. S.; Mortillo, S.; Jeyaseelan, R.; Kukral, D. W.; Fura, A.; Kamath, A.; Vyas, V.; Tokarski, J. S.; Barrish, J. C.; Hunt, J. T.; Lombardo, L. J.; Fargnoli, J.; Bhide, R. S. *J. Med. Chem.* **2005**, *48*, 3991.
13. Cumming, J. G.; McKenzie, C. L.; Bowden, S. G.; Campbell, D.; Masters, D. J.; Breed, J.; Jewsbury, P. *Bioorg. Med. Chem. Lett.* **2004**, *14*, 5389, and references therein.
14. Kamijo, S.; Kanazawa, C.; Yamamoto, Y. *J. Am. Chem. Soc.* **2005**, *127*, 9260.
15. Hynes, J., Jr.; Doubleday, W. W.; Dyckman, A. J.; Godfrey, J. D., Jr.; Grosso, J. A.; Kiau, S.; Leftheris, K. *J. Org. Chem.* **2004**, *69*, 1368.
16. Protocols for in vitro assays are as follows: p38 enzyme assays were performed in V-bottomed 96-well plates. The final assay volume was 60 μL prepared from three 20 μL additions of enzyme, substrates (MBP and ATP) and test compounds in assay buffer (50 mM Tris, pH 7.5, 10 mM $MgCl_2$, 50 mM NaCl, and 1 mM DTT). Bacterially expressed, activated p38 was pre-incubated with test compounds for 10 min prior to initiation of reaction with substrates. The reaction was incubated at 25 °C for 45 min and terminated by adding 5 μL of 0.5 M EDTA to each sample. The reaction mixture was aspirated onto a pre-wet filtermat using a Skatron Micro96 Cell Harvester (Skatron, Inc.), then washed with PBS. The filtermat was then dried in a microwave oven for 1 min, treated with MeltilLex A scintillation wax (Wallac), and counted on a Microbeta scintillation counter Model 1450 (Wallac). Inhibition data were analyzed by nonlinear least-squares regression using Prizm (GraphPadSoftware). The final

concentration of reagents in the assays are ATP, 1 μM; [γ-^{33}P]ATP, 3 nM, MBP (Sigma, #M1891), 2μg/well; p38, 10 nM; and DMSO, 0.3%.

TNF-α production by LPS-stimulated PBMCs: heparinized human whole blood was obtained from healthy volunteers. Peripheral blood mononuclear cells (PBMCs) were purified from human whole blood by Ficoll-Hypaque density gradient centrifugation and resuspended at a concentration of 5×10^6/mL in assay medium (RPMI medium containing 10% fetal bovine serum). 50 μL of cell suspension was incubated with 50 μL of test compound (4× concentration in assay medium containing 0.2% DMSO) in 96-well tissue culture plates for 5 min at rt. 100 μL of LPS (200 ng/mL stock) was then added to the cell suspension and the plate was incubated for 6 h at 37 °C. Following incubation, the culture medium was collected and stored at −20 °C. TNF-α concentration in the medium was quantified using a standard ELISA kit (Pharmingen-San Diego, CA). Concentrations of TNF-α and IC_{50} values for test compounds (concentration of compound that inhibited LPS-stimulated TNF-α production by 50%) were calculated by linear regression analysis.

17. (a) Liverton, N. J.; Butcher, J. W.; Claiborne, C. F.; Claremon, D. A.; Libby, B. E.; Nguyen, K. T.; Pitzenberger, S. M.; Selnick, H. G.; Smith, G. R.; Tebben, A.; Vacca, J. P.; Varga, S. L.; Agarwal, L.; Dancheck, K.; Forsyth, A. J.; Fletcher, D. S.; Frantz, B.; Hanlon, W. A.; Harper, C. F.; Hofsess, S. J.; Kostura, M.; Lin, J.; Luell, S.; O'Neill, E. A.; Orevillo, C. J.; Pang, M.; Parsons, J.; Rolando, A.; Sahly, Y.; Visco, D. M.; O'Keefe, S. J. *J. Med. Chem.* **1999**, *42*, 2180; (b) Fitzgerald, C. E.; Patel, S. B.; Becker, J. W.; Cameron, P. M.; Zaller, D.; Pikounis, V. B.; O'Keefe, S. J.; Scapin, G. *Nat. Struct. Biol.* **2003**, *10*, 764, Based on Ref. 17b the p38α binding mode from X-ray studies for a p38 inhibitor showing a preference for a (*S*)-α-methylbenzyl group is depicted below:.

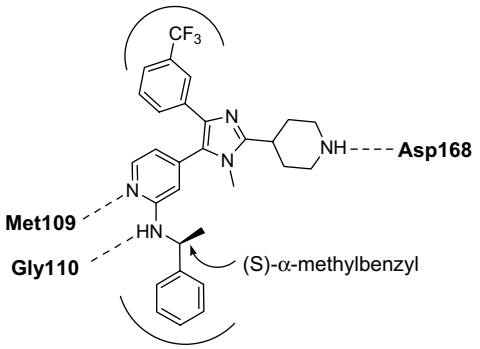

18. The gene encoding human p38α MAP kinase (isoform 2, residues 2-360) was subcloned into a pET28a vector (Novagen) between the NcoI and BamHI restriction sites, conferring expression of a noncleavable N-terminal pentahistidine-tagged enzyme. The resulting plasmid was used to transform a W3110 (DE3) strain of *E. coli* (American Type Culture Collection). Cells were grown at 37 °C into late log phase (OD_{600} of 11) in an oxygen-sparged 1-L fermenter using enriched Don's M101 medium [46 mM potassium phosphate, 23 mM ammonium sulfate, 4% (w/v) yeast extract (Becton Dickenson), 5% (w/v) Hy-Soy peptone (Quest Scientific), 2 mM magnesium sulfate, 2% glycerol (v/v), and 50 μg/mL kanamycin sulfate], chilled to 20 °C, and induced with 1 mM isopropyl β-D-thiogalactopyranoside (MP Biomedicals). Cells were harvested after 16 h by centrifugation at 5 °C and stored at −80 °C prior to purification. All purification steps were done at 4 °C, and were as follows. The cell paste from the culture expressing noncleavable pentahistidine-tagged p38α was lysed by homogenization at 8000–9000 psi (APV Rannie Mini-Lab 8.30H) in 25 mM Hepes, 500 mM NaCl, 50 mM imidazole, 5% glycerol (v/v), 2 mM β-mercaptoethanol, 1 μg/mL Leupeptin, and 1 μg/mL Pepstatin, pH 7.5. The lysate was clarified by ultracentrifugation (45 min at 30,000*g*) and filtration (1.2 μm syringe filter) before Ni-affinity chromatography (Pharmacia Biotech, Chelating Sepharose Fast Flow), eluting with an imidazole gradient from 50 to 500 mM final concentration in this buffer. Pooled fractions were dialyzed into 25 mM Hepes, 50 mM NaCl, 5% glycerol (v/v), 1 mM EDTA, 2 mM DTT, and 1 μg/mL Leupeptin, pH 7.5, and loaded onto a Pharmacia Resource Q anion exchange column followed by elution with a NaCl gradient to 0.6 M in the same buffer. Fractions containing target protein were combined and dialyzed into 25 mM Hepes, 200 mM NaCl, 5% glycerol (v/v), 1 mM EDTA, and 2 mM DTT, pH 7.5 and loaded onto a Pharmacia Superdex 200 (26/60) column and eluted with an isocratic gradient with the same buffer. The final fractions were combined and dialyzed into 25 mM Tris, 50 mM NaCl, 5% glycerol (v/v), 1 mM DTT, pH 7.4. Co-crystals of $(His)_5$-p38α 30 inhibitor complexes grew spontaneously in hanging drop vapor-diffusion trials conducted at 4 °C with drops containing 1 μL of concentrated protein–inhibitor complex mixed with an equal volume of reservoir solution (10% PEG 8000, 200 mM KCl, 100 mM MgOAc, 50 mM sodium cacodylate, pH 6.5). Prior to data collection, the crystals were slowly transferred to a stabilization solution (8% glycerol, 30% PEG 8000, 200 mM KCl, 100 mM MgOAc, 50 mM sodium cacodylate, pH 6.5) and then flash-frozen in liquid nitrogen. Data to 2.4 Å resolution were collected at the IMCA-CAT beamline BM-17 at the Advanced Photon Source, Argonne, IL. On a MarCCD detector, reduced with the programs DENZO and SCALEPACK, (Otwinowski, Z.; Minor, W. Processing X-ray data collected in oscillation mode. *Methods Enzymol.* **1997**, 276, 307–326.) and refined by program autoBuster (Global Phasing, Ltd, Cambridge, U.K.). The final crystallographic refinement R-factor was 21.2%. The coordinates have been deposited in the Protein Data Bank as entry 3BV2.

19. Pargellis, C.; Tong, L.; Churchill, L.; Cirillo, P. F.; Gilmore, T.; Graham, A. G.; Grob, P. M.; Hickey, E. R.; Moss, N. l.; Pav, S.; Regan, J. *Nat. Struct. Biol.* **2002**, *9*, 268.

20. Based on Ref. 13, the p38α binding mode for a quinazoline p38 inhibitor based on X-ray crystallography studies is depicted below:

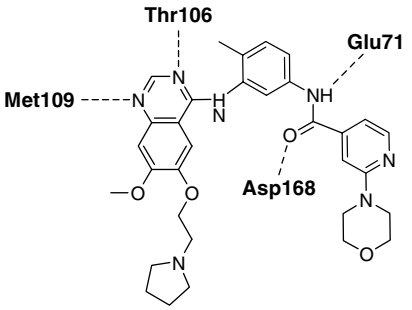

21. Wrobleski, S. T.; Doweyko, A. M. *Curr. Top. Med. Chem.* **2005**, *5*, 1005.